PROCEEDINGS, 50th Workshop on Geothermal Reservoir Engineering
Stanford University, Stanford, California, February 10-12, 2025
SGP-TR-229

Crush Resistance and Packing Strength of Candidate Proppant for Enhanced Geothermal Systems

Sree Sujon Sutradhor[1], Ahmad Ghassemi[1]

[1]Reservoir Geomechanics and Seismicity Research Group, The University of Oklahoma, Norman, OK 73069

ahmad.ghassemi@ou.edu

Keywords: Enhance Geothermal System, Hydraulic Fracturing, Proppant Strength, Ceramic Proppant, Petroleum-Coke Proppant.

ABSTRACT

Recent advancements in hydraulic fracturing technology have significantly improved the extraction of hydrocarbons and geothermal energy from unconventional reservoirs. This study evaluates the performance of various proppant materials, including petroleum coke-based proppants (PC), high-transported ultra-low-density ceramic proppants (LDC), and resin-coated ceramic proppants (RC), focusing on their crush resistance and packing strength under geothermal conditions. Utilizing the Standard procedure from API ISO 13503-2, we assessed both wet and dry proppants across two mesh sizes (10/35 and 35/60) and subjected wet samples to high temperatures (300 °C) for up to 30 days to simulate geothermal conditions.

The room temperature test results reveal that petroleum coke-based proppants, while cost-effective, exhibit lower strength compared to ceramic proppants. Whereas the resin-coated ceramic exhibited very high stress tolerance. Notably, the crush resistance and packing strength of proppants decreased with increasing temperature, with variations observed based on proppant type and size. Specifically, petroleum coke-based proppants did not show a significant decrease in strength after exposure to high temperatures. Conversely, ceramic-based proppants experienced a noticeable reduction in strength under the same conditions. In mixed proppant tests, blending PC with LDC or RC at various ratios showed a significant reduction in fines generation and improved mechanical performance, particularly at a closure pressure of 5000 psi, which is representative of geothermal reservoir conditions. These findings provide valuable insights into optimizing proppant selection and mixing for enhanced performance in both unconventional reservoirs and geothermal applications. The study highlights the importance of tailored proppant strategies to balance cost, strength, and efficiency, contributing to the development of more effective and economical fracturing solutions.

1. INTRODUCTION

In recent decades, advances in hydraulic fracturing technology have enhanced production from unconventional oil and gas reservoirs, as well as from geothermal resources (King, 2010; Montgomery & Smith, 2010). As most geothermal fields are in formations that consist of igneous and metamorphic rock with low permeability, it requires different stimulation techniques to extract heat energy efficiently. Due to high in-situ compressive stress, the fracture tends to close and result in permeability reduction. To avoid the closure of fractures, proppant is inserted into the fracture to withstand the in-situ force and keep the fracture open. Proppants are granular materials, usually sand or ceramic particles, that are injected into fractures to keep them open and so increase hydrocarbon flow from the reservoir to the wellbore. When proppants are placed between cracks, they tend to form a proppant pack and fluid can flow through their porous volume and in channels around distributed packs (Liu & Ghassemi, 2024). The appropriate selection and evaluation of proppants is a crucial factor that has a considerable influence on the efficacy of hydraulic fracturing. Proppant cost, density, and strength are key factors to consider when selecting proppant, especially in practical applications where significant quantities of proppant must be mixed with water and injected into the field. Among the wide array of proppants used, petroleum coke proppants have gained significant attention in recent times due to their notable advantages in terms of being lightweight and cost-effective. The most important parameter of hydraulic fracturing is the conductivity of the fracture which is defined as the multiplication of fracture permeability with fracture width. The width of the producing fracture varies with closure stress, amount of proppant within the fracture, proppant strength, and formation hardness (Mcdaniel & Services, 1986). The overall strength of the proppants is assessed by evaluating two critical parameters: crush resistance and packing strength. Crush resistance is defined as the maximum amount of stress that a proppant can withstand before producing more than 10% fines. It essentially assesses the proppant's capacity to endure the in-situ stress within the fracture without breaking down into fine particles that could diminishes the fracture permeability. Packing strength, on the other hand, refers to the proppant's ability to sustain fracture width under in-situ stress circumstances (Ko et al., 2023). To ensure the efficient and sustainable development of these resources, proppant crush testing has emerged as a pivotal area of research, offering insights into the mechanical behavior and performance of petroleum coke proppants under downhole conditions. To most important mechanical parameters of a proppant should be considered before selecting a proppant: proppant crush resistance (which is also known as K value) and proppant packing strength. The mechanical properties, including crush resistance and packing strength, exhibit significant variability depending on the test conditions and the size of the proppant (Bandara et al., 2021; Palisch et al., 2010). It is important to note that the crush resistance of dry proppant differs from that of wet proppant of the same size and other relevant parameters (Simo et al., n.d.; Zheng et al., 2018). Furthermore, even when conducting tests under identical conditions using the same proppant material, the strength of the proppant greatly varies with its size (Ko et al., 2023). Consequently, comprehensive testing involving different conditions and diverse size distributions of proppant is essential for obtaining thorough insights to aid in the selection of the most suitable proppant.

In this Experimental work, the Standard procedure provided by American Petroleum Institute (API) ISO 13503-2 (RP, A. 2008).) is modified to determine the crush resistance of the proppant. Similar to Ko and Ghassemi (Ko et al., 2023) the acoustic emission data emitted from the crushed cell due to crushing is collected and used to estimate the packing strength of the proppant. In this study, we evaluated the crush strength and packing strength of three distinct proppant materials: petroleum coke-based proppants (PC), high-transported ultra-low-density ceramic proppants (LDC), and resin-coated ceramic proppants (RC). The tests were conducted on both wet and dry proppants to assess the changes in packing strength and crush resistance under varying conditions. We tested two mesh sizes (10/35 and 35/60) for each type of proppant. To investigate the impact of high temperatures on the mechanical properties of the proppants, wet crush tests were performed on samples subjected to a high temperature of 300 °C for 7 and 14 days. These experimental results offer valuable insights into the behavior of proppant packs in Enhanced Geothermal Systems (EGS) at approximately 300 °C, contributing to the design of advanced proppants for geothermal applications. Additionally, Scanning Electron Microscopy with Energy Dispersive X-ray Spectroscopy (SEM-EDX) analysis was conducted to observe surface structure changes after heat exposure. Given that petroleum coke-based proppants are cheaper and weaker compared to ceramic-based proppants, we also performed crush tests on mixtures of PC with LDC and RC at varying ratios. These mixed proppant tests were carried out at a fixed pressure of 5000 psi (34.5 MPa) to determine the most economical and effective mixing ratio for field injection. We selected 5000 psi as the test pressure because it is the most common reservoir pressure encountered in field conditions. By analyzing stress-strain data and crush percentages across different mixing ratios, we can propose optimal mixing ratios for practical applications.

2. SAMPLE PREPARATION AND MATERIAL PROPERTIES

Three distinct proppant materials: petroleum coke-based proppants (PC), high-transported ultra-low-density ceramic proppants (LDC), and resin-coated ceramic proppants (RC) were prepared for the test. Before running the crush resistance test, elemental composition, bulk density, sphericity, and roundness were first characterized. As the strength of the proppant varies with the size of the proppant, in this study, two distinct size distributions of all three types of proppants have been tested to assess their suitability for use in hydraulic fracturing to keep the fracture open by resisting closure pressure. The proppant samples were sieved using a RO-TAP RX-29 sieve shaker. We used two different mesh sizes for our experimental analysis: 10/35 (with particle sizes ranging from 2000 to 500 microns) and 35/60 (with particle sizes falling between 500 and 250 microns). These sample sizes were chosen due to their ample availability, ensuring we had enough to carry out the test. According to the guidelines prescribed in ISO 13503-2, raw proppant samples were shaken for 10 minutes by a sieve shaker. Following the sieving, two desired-size distributed samples were collected to be used in the crush test. After sieving, the average bulk density of the proppant of each size distribution was measured. According to ISO 130503-2, the proppant concentration 4 lb/ft2 was used. The mass of proppant (m_p) needed for each test is then calculated using the equation $m\_p=24.7\times\rho\_bulk$. For the mixed testing, samples were prepared by combining proppants in various weight ratios: 1:3, 1:1, and 3:1. Specifically, the mixtures included 25% PC with 75% LDC, 50% PC with 50% LDC, 75% PC with 25% LDC, 25% PC with 75% RC, 50% PC with 50% RC, and 75% PC with 25% RC. In the context of proppant usage in well stimulation, the bulk density of the proppant plays a crucial role in determining the necessary mass of proppant to be injected into the well, and it also determines how far proppant will travel. Proppant with smaller bulk density will go far from the injection point whereas heavier proppant will settle close to the injection point (Liu & Ghassemi, 2024). Moreover, the bulk density value serves as a key parameter for calculating the required sample mass for testing within the crush cell. Density measurement data and proppant shape are given below in Table-1. The shape of the proppants was determined by visual estimation based on the chart given by iso standard (RP, A. 2008).

Table-1: Density Measurement and the shape of Proppants of Various Sizes.

Type of proppant	Sizes	Bulk Density (gm/cc)	Proppant shapes (X= Roundness, Y= sphericity)
Pet coke	10/35	1.09	(0.7,0.7)
	35/60	0.99	(0.3,0.5)
LDC	10/35	1.21	(0.9,0.9)
	35/60	1.27	(0.9,0.9)
RC	10/35	1.6	(0.9,0.9)
	35/60	1.53	(0.9,0.9)

2.1 Resin-coated ceramics (RC) and Ultra Low-Density Ceramic (LDC)

The higher-strength Carbo Ceramics's CARBOBOND LITE resin-coated high-performance ceramic proppant is designed for effectiveness at greater well depths and stresses. CARBOBOND LITE resin-coated is designed with high cyclic loading tolerance, while the bonded proppant pack is for reducing the effective stresses acting on the grains. The SEM-EDX analysis in Table-2 shows it consists of 61 % carbon, 12.4% nitrogen, and 24.2 % Oxygen. The bulk density of RC 10/35 proppant is 1.6 gm/cc and 1.53 gm/cc for RC

35/60. The scanning electron microscope (SEM) image shows that the proppant surface doesn't have any noticeable micro-cracks in it before exposed high temperature as shown in Figure-1 (left).

CARBOAIR high-transport, ultra low-density ceramic proppant technology enables operators to efficiently inject proppant at the long fracture. One of the key advantages of this proppant is that it can travel a long distance as the density is low, and it's much stronger compared to the petroleum coke-based proppants. The SEM-EDX analysis in Table-2 shows it consists of 69.3 % carbon, 27.6 % Oxygen, and trace number of other molecules. The bulk density of LDC 10/35 proppant is 1.21 gm/cc and LDC 35/60 is 1.27 gm/cc. The scanning electron microscope (SEM) image shows that the proppant surface doesn't have any noticeable micro-cracks in it before exposed high temperature as shown in Figure-1 (right).

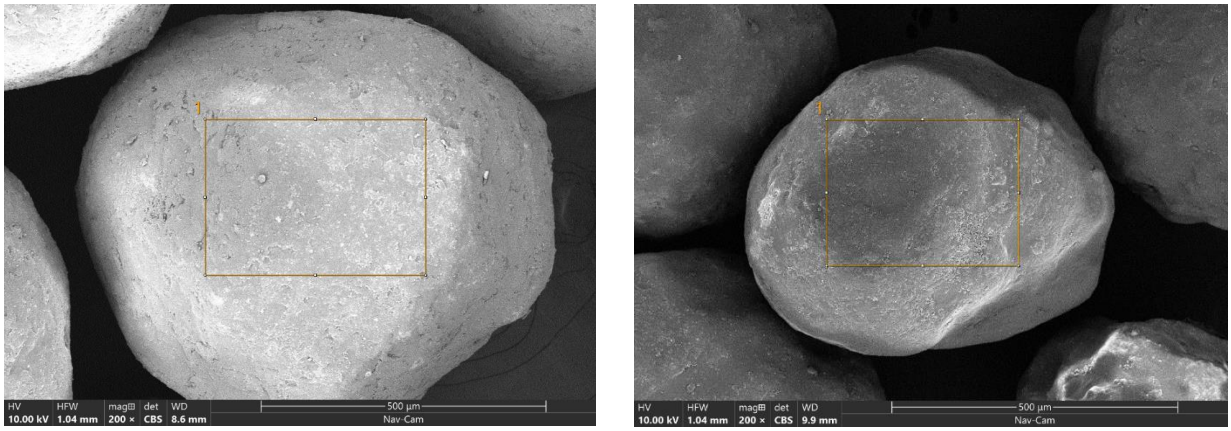

Figure-1: SEM image of resin-coated ceramic proppant of 10/35 mesh size (left). Right: SEM image of ultra-low density ceramic proppant of 10/35 mesh size

Table-2: SEM-EDX report of resin-coated ceramic and ultra-low density ceramic proppants.

Resin-Coated Ceramics			Ultra-Low Density Ceramics		
Element	**Atomic %**	**Weight %**	**Element**	**Atomic %**	**Weight %**
C	60.9	45.3	C	69.3	51.1
N	12.4	10.8	O	27.6	27.1
O	24.2	24.0	Na	0.5	0.7
Al	0.5	0.8	Al	0.3	0.4
Si	0.5	0.9	Si	0.3	0.5
Ir	1.5	18.3	Cl	0.5	1.1
			Ir	1.6	19.0

2.2 Petroleum-Coke Proppant

Petroleum Coke is a carbon-rich material derived from oil refining processes and is often used for fuel or aluminum manufacturing. Coke is a material obtained from the pyrolysis of hard coal carried out at a temperature of approximately 1000 °C (Suponik et al., 2023). The structure of the Coke proppant limits its embedment. The SEM-EDX analysis shows it consists of 96 % carbon and 3.67 % sulfur. The scanning electron microscope (SEM) image shows that the proppant has few micro-cracks in it before applying any stress. The presence of microcracks (Figure-2) will lead the proppant to fail at low stress. Petroleum coke proppants are well-known for their relatively low density and low price. When paired with low-viscosity foams and fracking fluids, this intrinsic feature allows them to be used more efficiently (Labus et al., 2019; Suponik et al., 2023). Furthermore, the low bulk and specific densities of coke proppants allow for the injection of large volumes of proppant from a single well into remote regions of the fractures. Petroleum coke proppant has a bulk density value that is nearly half that of sand. One main drawback of petroleum coke-based proppant is that they are relatively weak which make them less effective in keeping the fracture open.

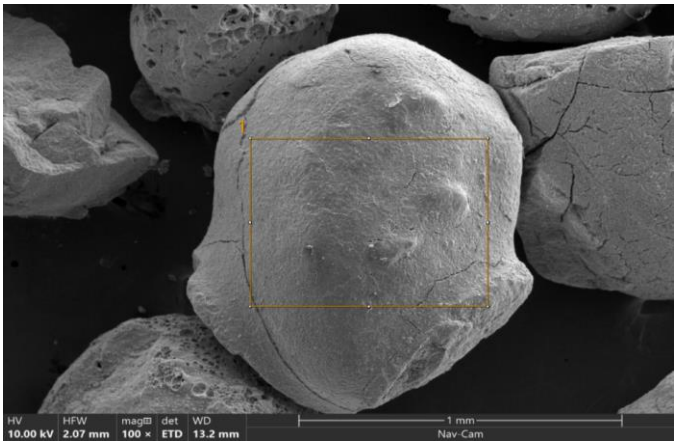

Element	Atomic %	Weight %
C	94.3	71.4
Al	0.2	0.3
Si	0.1	0.2
S	3.6	7.4
Ir	1.7	20.8

Figure-2: SEM image of 10/35 petroleum coke proppant with EDX analysis showing elemental composition.

3. METHODOLOGY

3.1 Dry Test Procedure

The standard crush test procedure provided by ISO 130503-2 is being followed to conduct the test. In this proppant crush testing procedure, the first step involves sieving the proppant and separate them based on their size distribution. The bulk density is then measured, and the required proppant mass for each test is calculated using the prescribed equation, maintaining a concentration of 4 lb/ft². The test cell is carefully loaded to form a consistent loose pack with a level surface. The piston is gently inserted without additional force and rotated 180° clockwise to ensure surface uniformity.

$$m_p = 24.7 \times \rho_{bulk} \quad (1)$$

Where m_p is the mass of proppant required, ρ_{bulk} is the bulk density.

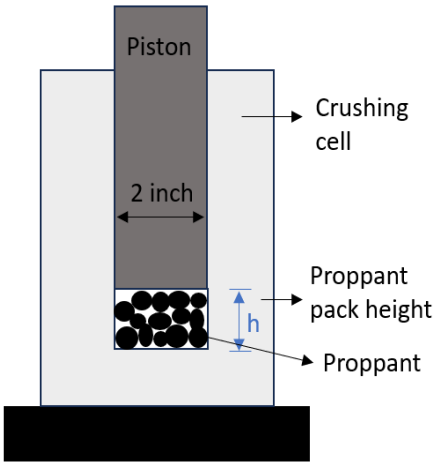

Figure 0.1: Schematic diagram of proppant crush cell assembly.

Hydraulic load frame with the capacity to apply very high load is used for this test to crush the proppant. In addition to ISO standard procedure, we also incorporated AE sensors to collect the AE response when the sample is crushing. The cell is placed beneath the loading piston of the MTS loading frame, ensuring its central positioning for uniform load distribution. For the crush test, the appropriate stress is applied to the test-cell piston at a constant rate of 2,000 psi/min, resulting in an applied load of F = 2000 * 3.1416 = 6283 lbf per minute, considering the piston's 2-inch diameter (with an area of 3.1416 inch^2). When the final stress level is achieved, the stress level is held for 2 minutes before being released. After crush testing, the proppant mass is re-screened to determine the percentage of fines generated due to the applied stress. Any particles smaller than the initial size of the proppant are categorized as fines. This test is repeated for the new sample of the same size with the final stress increment of 1000 psi until the percentage of fines generates exceed 10%. The "K-value" is determined as the maximum stress level attained during the testing process without exceeding 10.0% fines generation. This comprehensive procedure provides critical insights into the proppant's mechanical behavior, crush resistance, and packing strength, aiding in the selection and optimization of proppant materials for hydraulic fracturing and other applications. For the mixed proppants, a final stress of 5000 psi was applied to all samples using a hydraulic load frame at a loading rate of 2000 psi/min.

Once the target stress level was reached, it was maintained for 2 minutes before being released. After the crush testing, the proppant mass was re-screened to quantify the percentage of fines generated due to the applied stress.

3.2 Heated Test (Wet Test) Procedure

To replicate the high-temperature conditions of Enhanced Geothermal Systems (EGS) in the laboratory, the proppant material was subjected to heating using tap water at a temperature of 300°C. The water-immersed proppant was placed into a specialized vessel capable of withstanding high pressure and temperature conditions, and then the vessel was plugged tightly to prevent steam leakage. In our experiment, we used normal tap water. Figure 3(a) shows the pressure vessels that were used to heat the proppant, Figure-3(b) shows conceptual inside view of the vessel. Then the vessel was inserted into the oven at 300°C for 7, 14, and 30 days separately. Once the desired heating duration was reached, the vessel was allowed to cool down in water to ensure a controlled cooling process. After the vessel had sufficiently cooled, it was unplugged, and the interior was inspected for the presence of water. If the water inside the vessel had completely evaporated, indicating potential leakage, the experiment was repeated using new samples to ensure accurate and reliable results.

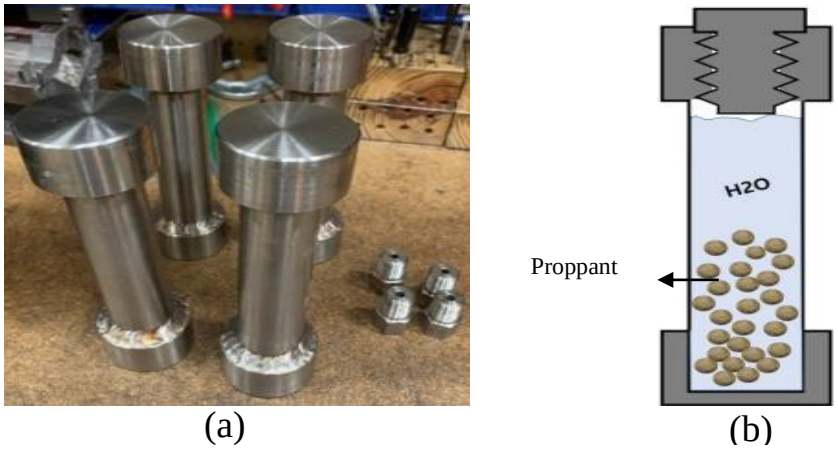

Figure-3: Pressure vessel used for heating proppants with water, b) inside view of the vessel.

After the heating process, the proppant and water contained within the vessel were carefully transferred to a testing cell, where a wet crush test was performed to evaluate the proppant's crush resistance in a saturated state. Following the test, the crushed sample was collected and left open at room temperature for 2–3 days to ensure complete drying. Once dried, the total mass of the crushed sample was recorded prior to sieving to account for any potential mass loss incurred during the heating and transfer processes. The dried, crushed samples were subsequently sieved to quantify the percentage of fines generated under the applied stress. Since the proppants remained immersed in water during the heating process and the crush tests were conducted while they were still in a wet state, this heated test is classified as a wet test.

3.2 Acoustic Emission Data Collection

Acoustic emissions (AE) refer to elastic waves generated when a material or structure experiences sudden fracturing or frictional sliding along discontinuities and grain boundaries (Mogi, K., 2006). AE testing is a well-established nondestructive testing (NDT) technique used to identify and pinpoint microcracks in structures and components under mechanical loading. However, the accuracy of AE data can be affected by background noise, which consists of unwanted signals captured by the sensors (Rens et al., 1997). A data filter was applied to eliminate low to mid-amplitude noise that could have been caused by frictional sliding between proppants. In this study, AE was filtered by amplitude of the signals, where amplitude lower than 60 dB considered as noise, and hence has been removed. An AE system generally consists of various components, including a sensor, preamplifier, filter, amplifier, display, and data storage units. In this study, two AE sensors were positioned near the bottom of the crushed cell to gather soundwave data emitted by the proppant during loading. AE data were captured using AEwins software by MISTRAS Group. The collected AE data is instrumental in understanding the proppant's response to stress. Acoustic emission (AE) data were collected by connecting two AE piezoelectric transducers to the side of the crushed cell near the bottom. In this study, two PZT (Piezoelectric Transducer) AE sensors with frequency band range is between 25kHz ~ 750kHz were positioned near the bottom of the crushed cell to gather soundwave data emitted by the proppant during loading.

As the proppant grains are crushed during the crush test, acoustic emissions are generated and recorded, containing vital information such as frequency, amplitude, count, AE hit rate, and so on. The acoustic emission data is then analyzed to determine the packing strength of the proppant. The acoustic emission (AE) measurements were post-processed and synchronized with the hydraulic load frame stress profile and displacement profile. Post-processing was accomplished using Python and Excel. Notably, there is a noticeable reduction in the hit rate of the proppant pack after undergoing significant crushing, indicating the attainment of a critical stress level that closely approximates the strength of the proppant packing (Ko et al., 2023). This deflection in hit rate becomes evident even before the target stress value selected for the crush resistance test is reached. The deflection of the AE hit rate indicates that the proppant has reached its ultimate packing strength. The AE rate plot was synchronized with the stress plot over time to estimate the packing strength of the proppant.

4. RESULT AND DISCUSSION

4.1 Dry Test Result

A series of crush experiments were performed under different settings with two different proppant sizes, namely 10/35 mesh and 35/60 mesh. These tests were conducted in both wet and dry conditions in order to fully assess their performance. During the phase of dry testing, the significant frictional contacts among the proppant grains resulted in a notable amount of undesired noise in the acoustic emission (AE) data. To address this issue, the AE data was subjected to a filtering process to remove the noise from the raw data. Amplitude values less than 70dB were disregarded from the analysis since they were deemed to be noise. As the crushing rate of proppant increases with the increasing applied stress, the number of hits also exhibited a corresponding rise as proppant crush. However, after a certain stress, the number of hits started decreasing, indicating that the applied stress had exceeded the critical stress limit. Figure 3.10 depicts the hit rate, stress, and displacement over time for 10/35 dry proppant. This decrease in the number of hits was observed at approximately 110 seconds, indicating that the proppant had undergone severe crushing and had reached the critical stress level. From Figure-4 (left), synchronizing the stress plot with hit rate plot, the applied stress at 110 seconds was measured at 2100 psi. For the dry proppant of size 35/60, shown in Figure-4 (right), the AE rate started to drop at 110 seconds, the applied stress at 110 seconds was measured at 1800 psi.

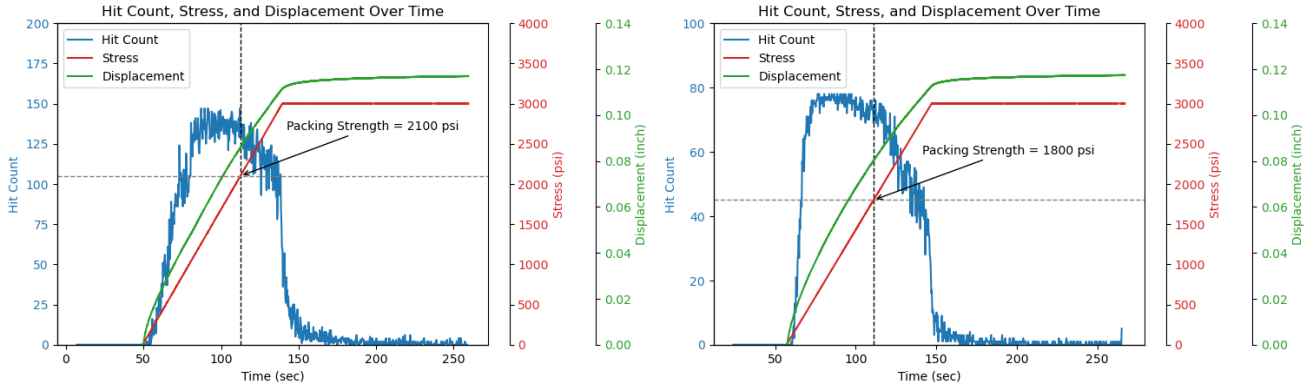

Figure-4: AE hit rate, applied stress, and displacement with respect to time during the crush test of petroleum coke-based (PC) proppant of size 10/35 (left) and 35/60 (right).

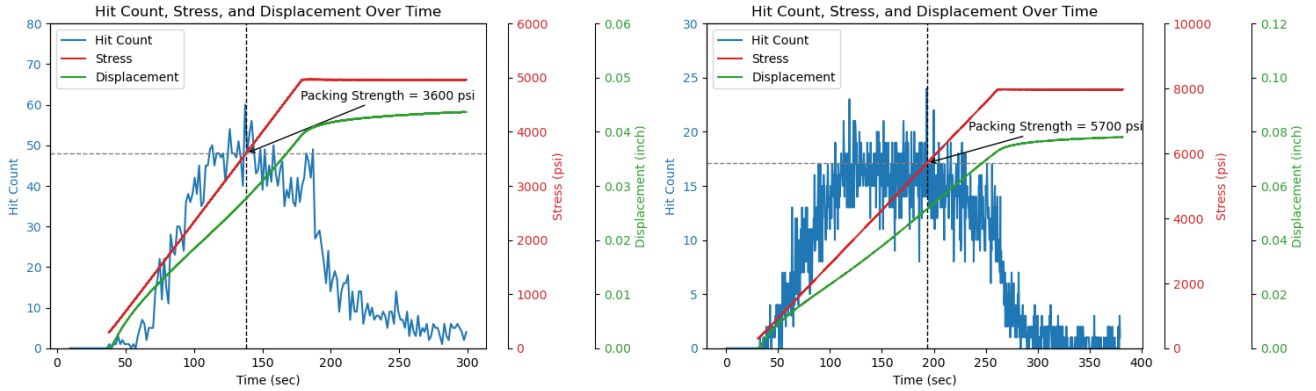

Figure-5: AE hit rate, applied stress, and displacement with respect to time during the crush test of ultra low-density (LDC) proppant of size 10/35 (left) and 35/60 (right).

Figure-5 illustrates stress, strain, and Acoustic Emission (AE) hit count response of LDC proppants with 10/35 mesh and 35/60 mesh sizes, respectively, over time. By correlating the AE hit count with the stress profile, it was determined that the packing strength of the LDC 10/35 mesh proppant is approximately 3600 psi, while the packing strength for the LDC 35 /60 mesh proppant is approximately 5700 psi.

Figure-6 represents the stress, strain, and AE hit count response of RC proppants with 10/35 mesh and 35/60 mesh sizes, respectively, over time. The decline in the AE hit count indicates that the packing strength of the RC 10/35 mesh proppant is approximately 10,200 psi, while the RC 35/60 mesh proppant exhibits a packing strength of approximately 12,100 psi. Notably, when the final stress is reached and the load increment is halted, holding this stress level for two minutes results in a sudden peak in AE hit count, followed by a gradual decline. This phenomenon can be attributed to a change in loading rate, which induces relative movement and sliding among proppant grains. The transient increase in AE activity suggests micro-rearrangements within the proppant pack

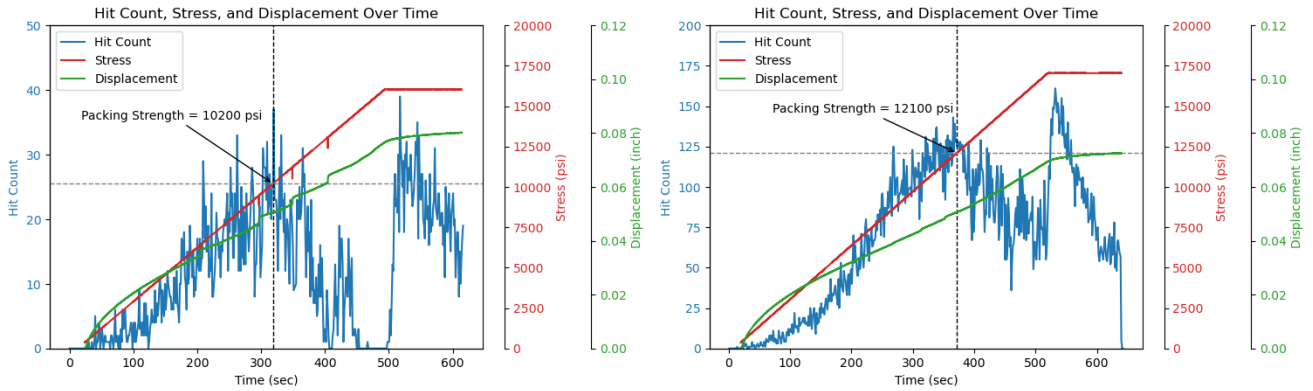

Figure-6: AE hit rate, applied stress, and displacement with respect to time during the crush test of resin-coated ceramic (RC) proppant of size 10/35 (left) and 35/60 (right).

Table 3 presents the crush resistance results for different proppants, focusing on their K-values, packing strengths, and the percentage of fines generated at the K-value. The K-value is a crucial measure that indicates the highest stress a proppant can withstand while producing less than 10% crushed fines. This parameter is key to understanding the durability and effectiveness of proppants under high-pressure conditions. The petroleum coke-based proppant (PC) is shown to be the weakest among the tested materials. For the 10/35 mesh size, the PC proppant has a packing strength of 2100 psi and a K-value of 2K, with 6.67% fines generated at this stress level. The 35/60 mesh size also exhibits a low packing strength of 1800 psi, with the same K-value of 2K, but with a slightly higher fines generation of 8.90%. These results suggest that PC proppants have limited capacity to withstand high pressures, making them less suitable for higher depth reservoir applications.

In contrast, the high-transported ultra-low density ceramic proppant (LDC) displays significantly higher strength and resistance. The 10/35 mesh size has a packing strength of 3600 psi and a K-value of 4K, and for the 35/60 mesh size, the packing strength is 5700 psi, and the K-value rises to 7K. These figures indicate that LDC proppants are much more robust compared to PC, making them better suited for environments with higher stress levels, and smaller size can withhold high stress.

The resin-coated ceramic proppant (RC) emerges as the strongest proppant tested. The 10/35 mesh size has an impressive packing strength of 10200 psi and a K-value of 15K. The 35/60 mesh size further increases in strength, with a packing strength of 12100 psi and a K-value of 17K. These results highlight the superior crush resistance of RC proppants, particularly in the finer 35/60 mesh size, making them ideal for extreme pressure environments such as high-stress hydraulic fracturing operations. This information is vital for selecting the appropriate proppant for specific applications, particularly in scenarios where high pressure and minimal fines generation are critical.

Table 0: K-value, packing strength, and percentage of fines generated at K-value for all types of proppants.

Proppant Type	Sizes	Packing strength (psi)	K-value	Fine generates at K-value (%)
PC	10_35	2100	2K	6.67
	35_60	1800	2K	8.90
LDC	10_35	3600	4K	7.77
	35_60	5700	7K	9.7
RC	10_35	10200	15K	7.5
	35_60	12100	17K	9.03

4.2. Heated Test Results

For the petroleum coke (PC) proppants, as shown in the plot, the percentage of fines generated remained relatively stable, with values of 6.67%, 7.88%, 8.23%, and 10.1% for the 10/35 size after 0, 7, 14, and 30 days of heat exposure, respectively. The 35/60 size PC proppants also showed minimal change, with fines percentages of 8.90%, 9.00%, 11.10%, 9.69% across the same time periods. This minimal variation suggests that PC proppants have relatively consistent performance under heat exposure, though they are inherently weaker compared to other proppants. Figure-7 and 8 shows the percentage of fines generated by each type of proppant with respect to the duration of time they were exposed to high temperatures.

In contrast, the LDC and RC proppants exhibited significant increases in fines generation with prolonged heat exposure, indicating a substantial loss in strength. For the LDC proppants, the 10/35 size showed fines percentages of 7.77%, 23.34%, 28.25%, and 36.01 while the 35/60 size showed 9.70%, 21.62%, 27.26%, and 26.06 fines for 0, 7, 14, and 30 days, respectively. This dramatic increase highlights the sensitivity of LDC proppants to high temperatures, particularly for longer exposure durations.

The RC proppants were even more affected by heat exposure. The 10/35 size proppants showed fines percentages of 7.50%, 28.47%, 38.04%, and 37.87, while the 35/60 size recorded 9.03%, 15.36%, 19.28%, and 18.40 fines after 0, 7, 14, and 30 days, respectively. The significant increase in fines, especially for the 10/35 size, demonstrates that RC proppants, despite their initial strength, experience considerable degradation when exposed to prolonged high temperatures. Overall, these plots emphasize the impact of heat exposure on proppant strength, with RC proppants showing the most significant degradation, followed by LDC, and PC proppants demonstrating the least change, albeit from a lower initial strength baseline.

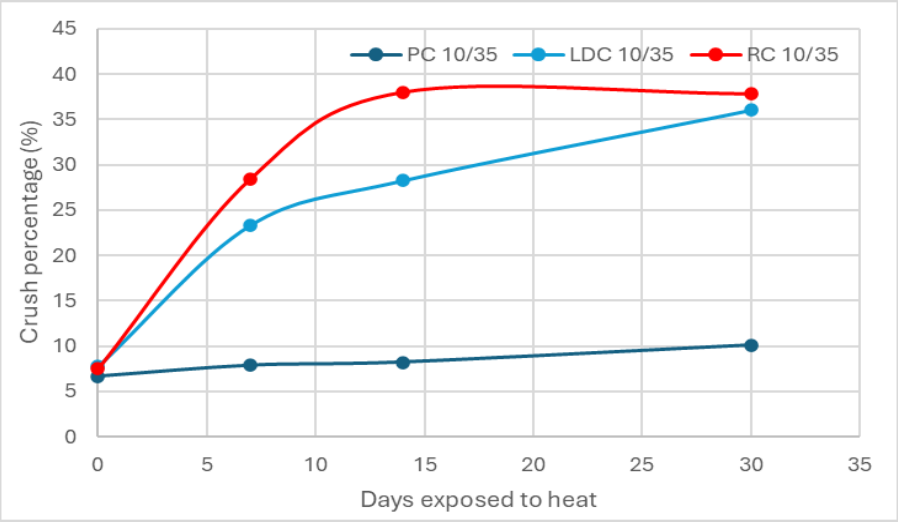

Figure-7: The percentage of fines generated for proppants of sizes 10/35 after being exposed to high temperatures for 0, 7, 14, and 30 days.

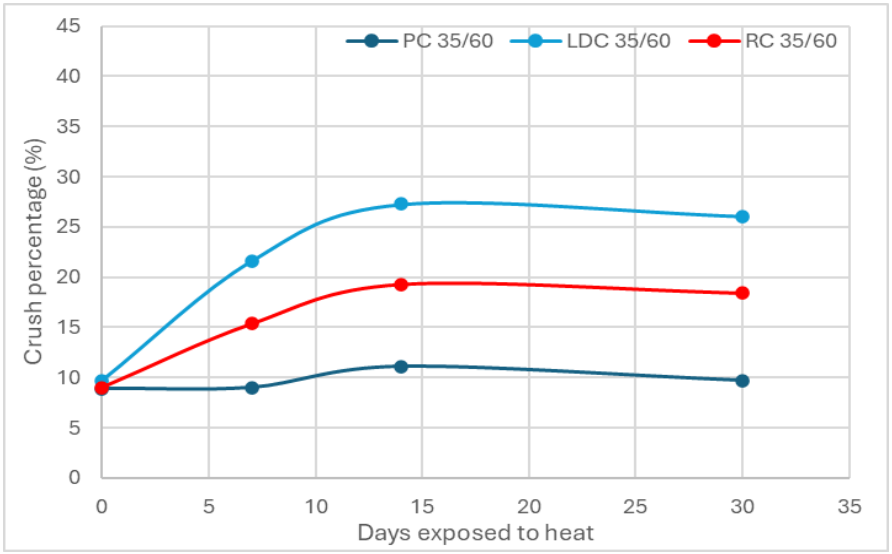

Figure-8: The percentage of fines generated for proppants of sizes 35/60 after being exposed to high temperatures for 0, 7, 14, and 30 days.

4.3 SEM Image Analysis of Heated Proppants

Scanning Electron Microscopy (SEM) is an imaging method used to examine surfaces and near-surface areas of solid specimens. It works by exploiting different interactions, including elastic and inelastic scattering, between an electron beam and the specimen's surface (Stachowiak, G., & Batchelor, A. W. (2004)). In our study, we analyzed the surface of intact proppants and the surface of proppants that were exposed to high temperatures (300C) for 7, 14, and 30 days separately. SEM image was able to show the changes has taken place in the surface of proppant after being exposed to heat. Figure-9 to Figure-12 shows the changes that were taken place on

the surface of the proppants as they were exposed to high temperatures (300C) for 7, 14, and 30 days separately. From all the SEM images, it's clear that ceramic proppants undergo through degradation, and it's related to the duration of high temperatures exposure.

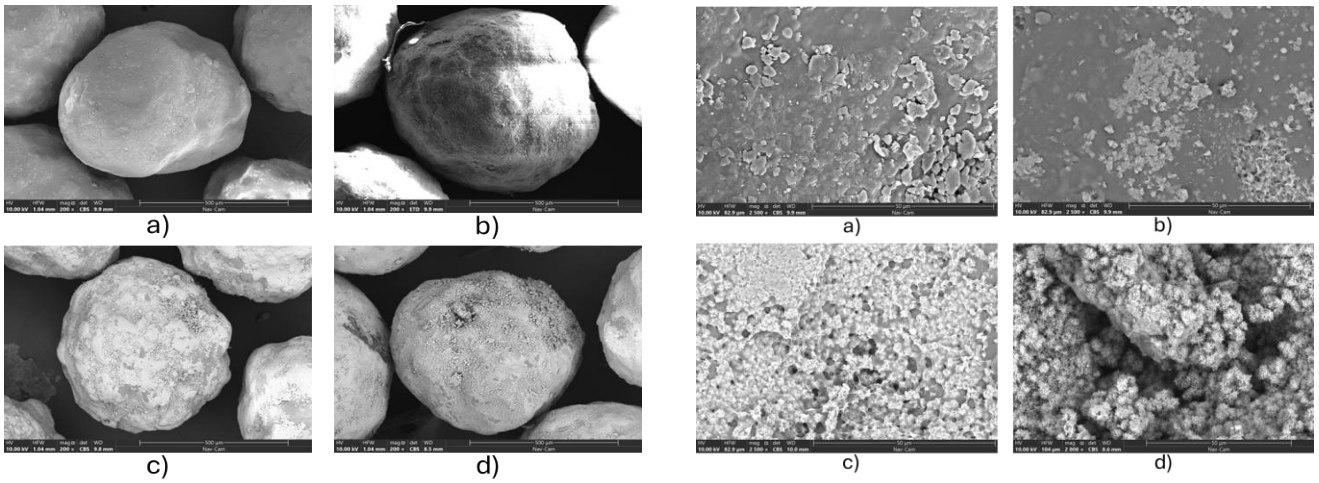

Figure-9: SEM images of LDC 10/35 proppants at 200x magnification. (a) Surface morphology of intact proppants, showing a smooth and unaltered structure. (b), (c), and (d) shows the surface of proppants that were exposed to heat for 7 days, 15 days, and 30 days, showing significant degradation with visible fractures and more pronounced surface roughness (Left). SEM images of LDC 10/35 proppants at 2000x magnification for clear inspection (right).

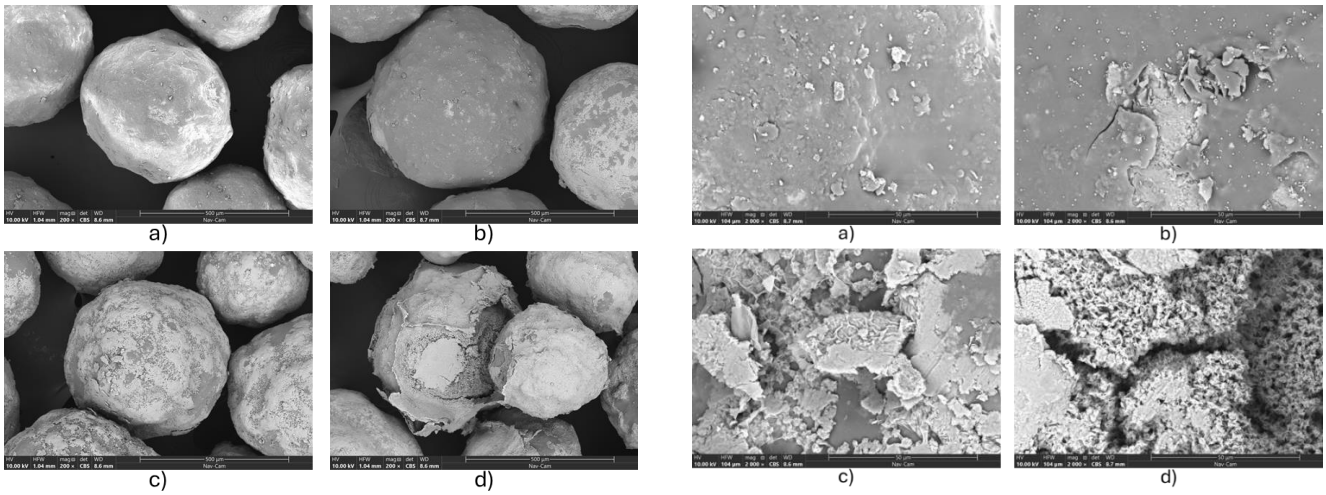

Figure-10: SEM images of LDC 35/60 proppants at 200x magnification. (a) Surface morphology of intact proppants, showing a smooth and unaltered structure. (b), (c), and (d) shows the surface of proppants that were exposed to heat for 7 days, 15 days, and 30 days, showing significant degradation with visible fractures and more pronounced surface roughness (Left). SEM images of LDC 35/60 proppants at 2000x magnification for clear inspection (right).

The SEM image analysis of LDC 10/35 and LDC 35/60 proppants at 200x and 2000x magnifications provides a detailed assessment of their surface morphology under prolonged high-temperature exposure (shown in figure-9 and 10). Initially, the intact proppants exhibit smooth surfaces without any visible microcrack, reflecting their mechanical integrity. However, after 7 days at 300°C, both proppant sizes show early signs of surface roughening and minor cracks, indicating the onset of thermal degradation. By 15 days, the degradation becomes more pronounced, with visible fractures, material disintegration, and the formation of scale on the surface. At 30 days, extensive damage is evident, characterized by deep cracks, and severe surface roughness, highlighting progressive weakening. The higher magnification images (2000x) reveal microstructural changes, including the formation of microcracks and surface scales, further supporting the correlation between thermal exposure and mechanical deterioration. The accumulation of scale with increasing exposure time is particularly concerning, as it can significantly reduce the fracture conductivity by obstructing fluid flow. Comparing both LDC 10/35 and 35/60, smaller size LDC experiences more surface degradation. These finding are consistent with the strength reduction observed in crush tests, confirming the adverse impact of prolonged high-temperature conditions on proppant durability.

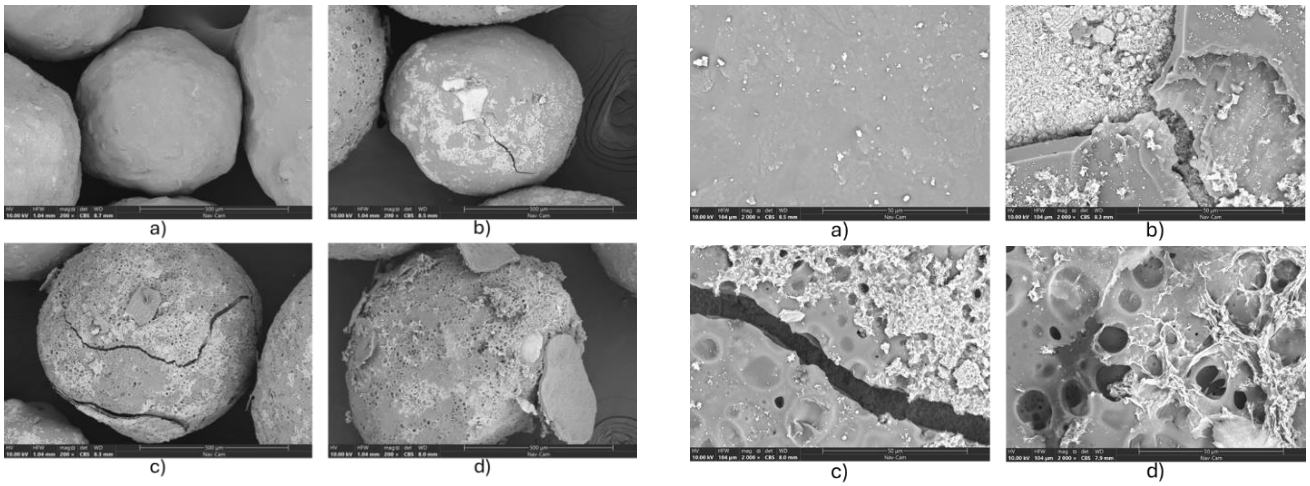

Figure-11: SEM images of RC 10/35 proppants at 200x magnification. (a) Surface morphology of intact proppants, showing a smooth and unaltered structure. (b), (c), and (d) shows the surface of proppants that were exposed to heat for 7 days, 15 days, and 30 days, showing significant degradation with visible fractures and more pronounced surface roughness (Left). SEM images of RC 10/35 proppants at 2000x magnification for clear inspection (right).

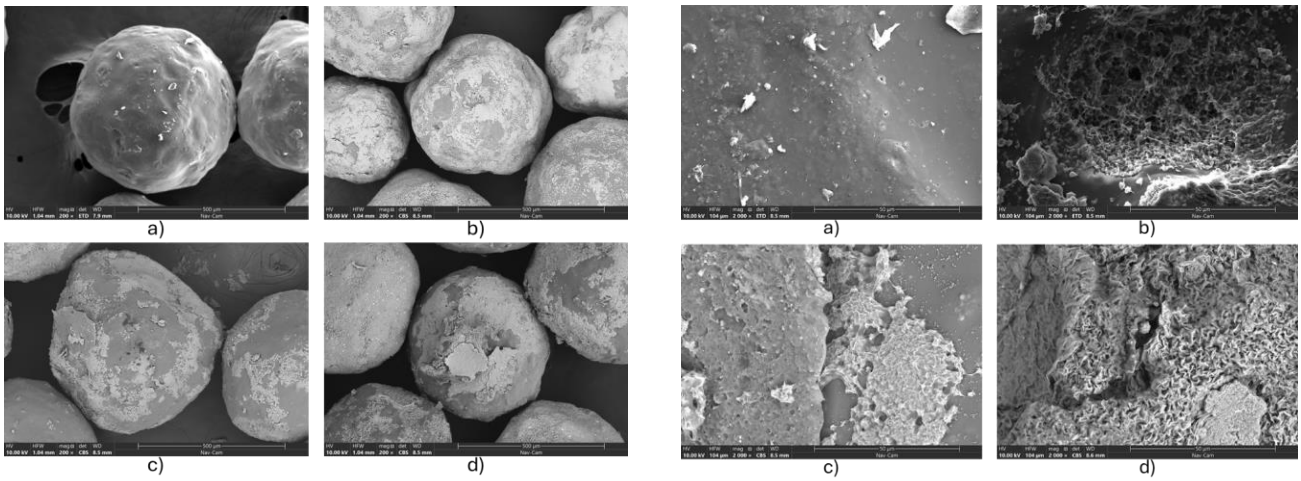

Figure-12: SEM images of RC 35/60 proppants at 200x magnification. (a) Surface morphology of intact proppants, showing a smooth and unaltered structure. (b), (c), and (d) shows the surface of proppants that were exposed to heat for 7 days, 15 days, and 30 days, showing significant degradation with visible fractures and more pronounced surface roughness (Left). SEM images of RC 35/60 proppants at 2000x magnification for clear inspection (right).

Figure-11 and 12 shows the SEM image analysis of RC 10/35 and RC 35/60 proppants at 200x and 2000x magnifications highlights the progressive deterioration of their surface coatings under extended high-temperature exposure, aligning with the crush test results. Initially, both proppant sizes exhibit a smooth and uniform coating, indicative of their structural stability. However, thermal exposure gradually weakens the coating, leading to crack formation and surface irregularities. Notably, RC 10/35 proppants display more pronounced surface damage, with deeper fractures and extensive coating degradation compared to RC 35/60. This observation is consistent with the higher crush percentage recorded for RC 10/35, confirming its greater mechanical degradation. These observations are consistent with the mechanical weakening seen in crush tests, confirming the adverse impact of prolonged high-temperature exposure on the proppants' durability and long-term performance in maintaining fracture conductivity.

4.3. Mixed Test Result

From the above results, it's clear that PC has very low strength as 2000 psi, on the other hand RC has high strength as 17000 psi. But the price of RC or LDC is much higher compared to the PC price, and in real field tons of proppants need to inject to keep the fracture open. To efficiently select proppants, we tried mixing LDC in PC, and RC in PC at different ratio to enhance their strength and make the proppant injection economically viable. The displacement curve is a crucial indicator in assessing the performance of proppants in hydraulic fracturing. It provides insights into how well a proppant can tolerate load during the fracturing process. Specifically, a lower displacement on the curve suggests that the proppant is less likely to compact under stress. This lower compaction translates to higher fracture conductivity, as the proppant remains more effective in maintaining open fractures and facilitating fluid flow. Figure 3.24

shows the how the proppant pack thickness changes with applied stress 5000 psi final stress at 2000 psi/min loading rate for different mixing ratio of PC with LDC. The plot shows that increasing the LDC content reduces the displacement, reflecting better performance in withstanding stress. The stress-strain curve on the left plot for the 50% PC - 50% LDC of 10/35 mesh size mixture demonstrates a clear reduction in compaction compared to 100% PC, but it is not as effective as the RC mix. On the right plot, the reduction in displacement is more apparent as LDC content increases. The plot indicates that the 25% PC - 75% LDC mix is particularly effective in minimizing displacement, suggesting strong reinforcement by LDC at this ratio.

The RC mixtures demonstrate a more pronounced reduction in net displacement compared to the LDC mixes. Figure 3.25 shows that even after mixing 25% RC with 75 % PC has greatly reduced the compaction compared to the 100% PC. This indicates a significant improvement in the mechanical strength of the proppant pack when mixed with RC.

Figure 3.26 illustrates the relationship between the percentage of proppant concentration (PC) and the percentage of fines generated. The plot reveals that the fines generated remain nearly constant across various mixing ratios for the 10/35 PC and LDC combinations. This stability in fines generation is attributed to the fact that both LDC and 10/35 PC have K-values (4k and 2k, respectively) that are lower than the applied stress of 5000 psi.

For all other cases, the crush percentage generated decreases significantly as the percentage of LDC or RC in the mixture increases. This indicates that incorporating LDC or RC into the PC mixture substantially reduces fines generation and enhances the proppant's resistance to compaction, leading to improved fracture conductivity and efficiency.

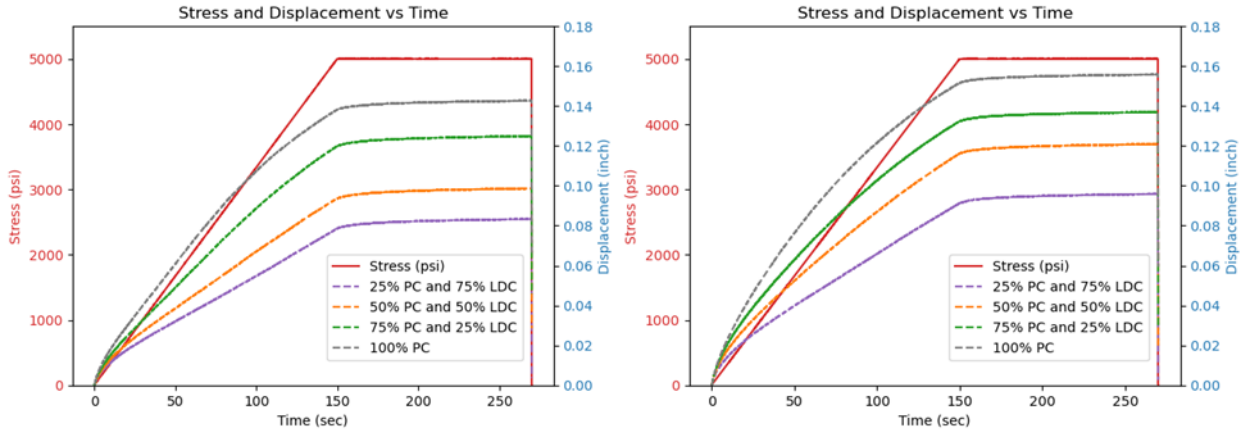

Figure 0.1: The stress and displacement response with respect to time for different mixing ratio of PC and LDC. The left figure shows the results for 10/35 mesh sizes and the right plot shows the results for 35/60 mesh sizes.

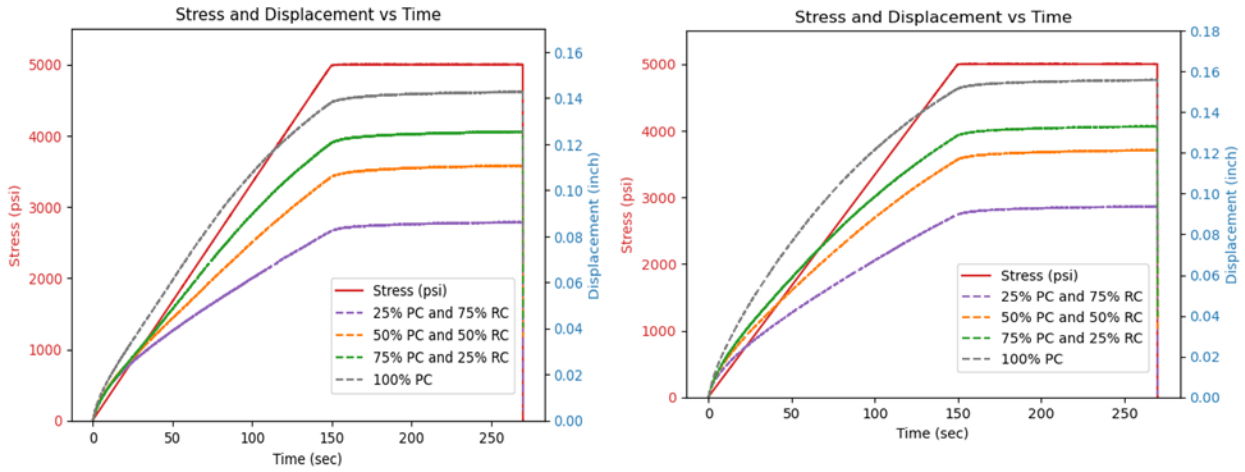

Figure 0.2: The stress and displacement response with respect to time for different mixing ratio of PC and RC. The left figure shows the results for 10/35 mesh sizes and the right plot shows the results for 35/60 mesh sizes.

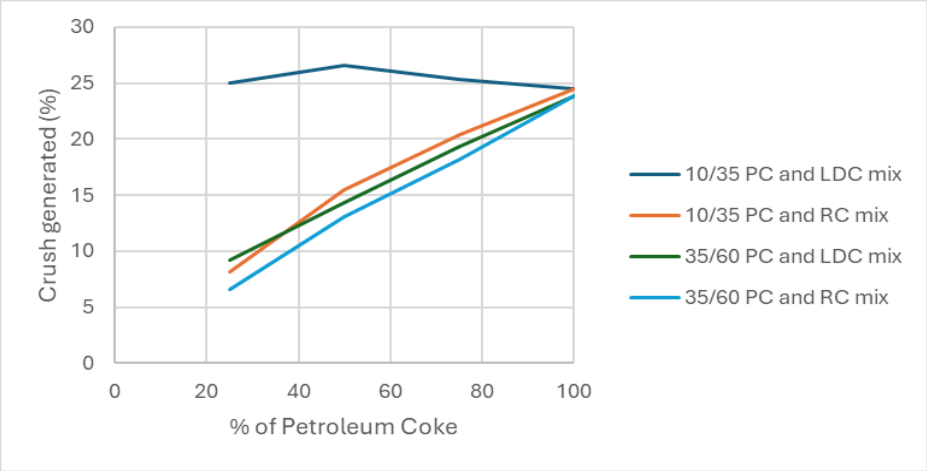

Figure 0.3: Crush generated with respect to the percentage of PC in the mixture, 5000 psi stress was applied in all mixture.

5. CONCLUSION

This study provides a comprehensive evaluation of the mechanical properties of various proppants under simulated downhole conditions. The findings demonstrate that while PC proppants are economically advantageous, they exhibit lower strength compared to ceramic-based alternatives. Among the ceramic proppants, RC proppants showed superior stress tolerance.

Temperature has a significant impact on proppant performance. The crush resistance and packing strength of all proppants decreased with rising temperatures; however, the extent of degradation was notably different between proppant types. PC proppants retained their strength even after exposure to high temperatures, whereas ceramic-based proppants experienced a substantial reduction in strength. The results underscore the importance of selecting appropriate proppants based on both economic considerations and performance requirements. For applications involving high temperatures, such as in geothermal systems, PC proppants might offer a more stable and cost-effective solution compared to ceramic proppants, which show more significant strength reduction under similar conditions. Further research and field testing are recommended to optimize proppant selection and mixing strategies for enhanced efficiency and cost-effectiveness in various fracturing scenarios

The SEM-EDX analysis of the proppants before and after heat exposure displayed noticeable changes in the surface structure. Microcracks were more prevalent in the proppant exposed to heat, and the presence of gas release pores was observed, suggesting potential alterations in the proppant's properties due to high-temperature conditions. The findings will contribute to the selection and optimization of proppant materials for efficient and sustainable development of unconventional oil and gas reservoirs, as well as geothermal fields.

6. ACKNOWLEDGEMENT

The authors sincerely appreciate the support provided by the OU Reservoir Geomechanics and Seismicity Group. The authors would like to thank Dr. Zhi Ye, Sunghyun Ko, and lab manager Steve for their invaluable assistance. This project was supported by the Utah FORGE project sponsored by the U.S. Department of Energy, through the project “Development and Testing of Tagged Proppant for Fracture Conductivity Enhancement and Reservoir Characterization in EGS”.

REFERENCES

Bandara, K. M. A. S., Ranjith, P. G., Rathnaweera, T. D., Wanniarachchi, W. A. M., & Yang, S. Q. (2021). Crushing and embedment of proppant packs under cyclic loading: An insight to enhanced unconventional oil/gas recovery. *Geoscience Frontiers*, *12*(6). https://doi.org/10.1016/j.gsf.2020.02.017

King, G. E. (2010, September). Thirty years of gas shale fracturing: what have we learned?. In SPE Annual Technical Conference and Exhibition? (pp. SPE-133456). SPE.

Ko, S., Ghassemi, A., & Uddenberg, M. (2023). Selection and Testing of Proppants for EGS. In *Stanford University*.

Labus, K., Morga, R., Suponik, T., Masłowski, M., Wilk, K., & Kasza, P. (2019, April). The concept of coke based proppants for coal bed fracturing. In IOP Conference Series: Earth and Environmental Science (Vol. 261, No. 1, p. 012026). IOP Publishing.

Liu, B., & Ghassemi, A. (2024). Simulation of proppant placement in multiple simultaneously propagating hydraulic fractures in horizontal wells. Rock Mechanics and Rock Engineering, 57(11), 9635-9650.

Mcdaniel, B. W., & Services, H. (1986). *SPE SPE 15067 Conductivity Testing of Proppants at High Temperature and Stress*. http://onepetro.org/SPEWRM/proceedings-pdf/86CRM/All-86CRM/SPE-15067-MS/2029159/spe-15067-ms.pdf/1

Mogi, K. (2006). Experimental rock mechanics. CRC Press.

Montgomery, C. T., & Smith, M. B. (2010). Hydraulic fracturing: History of an enduring technology. Journal of Petroleum Technology, 62(12), 26-40.

Palisch, T., Duenckel, R., Chapman, M., Woolfolk, S., Ceramics, C., & Vincent, M. C. (2010). *How To Use and Misuse Proppant Crush Tests: Exposing the Top 10 Myths*.

Rens, K. L., Wipf, T. J., & Klaiber, F. W. (1997). Review of nondestructive evaluation techniques of civil infrastructure. Journal of performance of constructed facilities, 11(4), 152-160.

RP, A. (2008). Measurement of Properties of Proppants used in Hydraulic Fracturing and Gravel-packing Operations. ANSI/API Recommended Practice 19c.

Stachowiak, G., & Batchelor, A. W. (2013). Engineering tribology. Butterworth-heinemann.

Simo, H., Pournik, M., & Sondergeld, C. H. (n.d.). *SPE 164506 Proppant Crush Test: A New Approach*. http://onepetro.org/SPEOKOG/proceedings-pdf/13POS/All-13POS/SPE-164506-MS/1562137/spe-164506-ms.pdf/1.

Suponik, T., Labus, K., & Morga, R. (2023). Assessment of the Suitability of Coke Material for Proppants in the Hydraulic Fracturing of Coals. *Materials*, *16*(11). https://doi.org/10.3390/ma16114083.

Zheng, W., Silva, S. C., & Tannant, D. D. (2018). Crushing characteristics of four different proppants and implications for fracture conductivity. *Journal of Natural Gas Science and Engineering*, *53*, 125–138. https://doi.org/10.1016/j.jngse.2018.02.028